International Journal of Sciences: Basic and Applied Research (IJSBAR)

ISSN 2307-4531
(Print & Online)

http://gssrr.org/index.php?journal=JournalOfBasicAndApplied

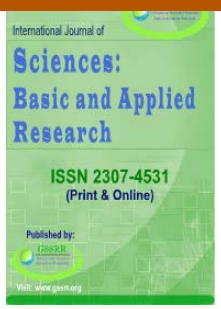

MHD Stability of a Streaming Resistive Hollow Jet Analytic and Numeric Analysis

Alfaisal A. Hasan[a]*, Alaa El-Din Abdin[b], Mostafa A. M. Abdeen[c]

[a]*Basic and Applied Sciences Department, College of Engineering and Technology, Arab Academy for Science & Technology and Maritime Transport (AASTMT), P.O. Box 11Aswan, Egypt*

[b]*National Water Research Center, Ministry of Water Resources and Irrigation, Egypt*

[c]*Department of Engineering Mathematics and Physics, Faculty of Engineering, Cairo University, Giza 12211,Egypt*

[a]*Email: alfaisal772001@gmail.com*

[b]*Email: alaa_ea_abdin@yahoo.com*

[c]*Email: mostafa_a_m_abdeen@hotmail.com*

Abstract

The axisymmetric magneto hydrodynamic (MHD) stability of streaming resistive hollow jet under oblique varying magnetic fields has been discussed. The stability criterion is established in its general form, studied analytically and the results are confirmed numerically. The destabilizing effect of the capillary force is found in small domain in the axisymmetric perturbation. Following the analytical solution and its effort, the Artificial Neural Network (ANN), one of the artificial intelligence techniques, was developed for simulating and predicting the stability of streaming resistive hollow jet. The results from the developed ANN models presented in this study showed that ANN technique, with less effort and time, is very efficiently capable of simulating and predicting the MHD stability of Streaming jet.

Keywords: Resistive fluid; Magneto hydrodynamic; Hollow Jet; Numerical simulation; Artificial Neural Network.

---

* Corresponding author.

1. Introduction

The stability analysis of a full fluid jet has been extensively studied by Chandrasekhar and Fermi [8]. More extensions along this problem and others acting upon different forces were studied by Chandrasekhar [7]. The stability of different cylindrical models under the action of self-gravitating force in addition to other forces has been elaborated by Radwan and Hasan [18,19]. Hasan [10] has studied the stability of an oscillating streaming fluid cylinder subject to the combined effect of the capillary, self-gravitating and electro dynamic forces in all modes of perturbation. He [11] has studied the instability of an oscillating streaming self-gravitating dielectric incompressible fluid cylinder surrounded by tenuous medium of negligible motion pervaded by transverse varying electric field for all modes of perturbation. He [12] has studied the instability of a full fluid cylinder surrounded by self-gravitating tenuous medium pervaded by transverse varying electric field under the combined effect of the capillary, self-gravitating and electric forces for all modes of perturbation. He [13] has discussed magnetohydrodynamic stability of a fluid jet pervaded by transverse varying magnetic field. Hasan and Abdelkhalek [14] has studied the magneto gravity dynamic stability of a streaming fluid cylinder and examining the influence of capillary and magnetic forces on the self-gravitating instability of the present models. This may be carried out, for all axisymmetric and non-axisymmetric modes of perturbation. Hasan [15] has studied the linear stability of self-gravitating compound dielectric immiscible jets under the influence of an axial electric field.

Since the analytic techniques need a lot of effort and time, the need for utilizing new methodologies and techniques to reduce this effort and save time (and at the same time preserving high accuracy) is urged. Artificial intelligence has proven its capability in simulating and predicting the behavior of the different physical phenomena in most of the engineering fields. Artificial Neural Network (ANN) is one of the artificial intelligence techniques that have been incorporated in various scientific disciplines. Abdeen [2] developed neural network model for predicting flow characteristics in irregular open channels. In [3] Abdeen presented a study for the development of ANN models to simulate flow behavior in open channel infested by submerged aquatic weeds. In [4] he predicted the Impact of vegetations in open channels with different distributeries. Hodhod and Abdeen [16] predicted the effect of natural and steel fibers on the performance of concrete using artificial neural networks. Gaafar and his colleagues [9] investigated the acoustic properties of some Tellurite glasses using artificial intelligence technique. In [5] Abdeen and Hassan studied MHD stability of streaming jet analytically and numerically using artificial intelligence technique. In [6] Abdeen and Bichir studied the deflection behavior of simply supported thin FGM rectangular plate resting on fluid layer using ANN. El-Mallawany and his colleagues [17] simulated the acoustic properties of some Tellurite glasses using ANN technique.

In all previous works, the fluid is assumed to be perfectly conducting and the resistivity of the magnetized fluid is neglected. In the present work, the axisymmetric MHD stability of a resistive hollow jet cylinder with oblique varying magnetic field is discussed analytically. Numerical simulation technique is adopted to develop a simulation model able to simulate and predict the MHD stability of a resistive hollow jet without the need to go through the presented analytic solution.

2. Analytic Formulation

Consider a gas cylinder (of negligible motion) of radius R_o as shown in figure 1, surrounded by a non-viscous, incompressible and resistiveliquid moving with uniform velocity

$$\underline{u}_o = (0,0,U) \tag{1}$$

The interior cylinder is being a gas with constant pressure P_o^g and pervaded by an oblique varying magnetic field

$$\underline{H}_o^g = \left(0, \frac{\beta\, r H_0}{R_0}, \alpha\, H_o\right) \tag{2}$$

The liquid is penetrated by the magnetic field

$$\underline{H}_0 = (0,0,H_o) \tag{3}$$

Where H_o is the intensity of the magnetic field in the liquid and β, α are some parameters satisfying certain restrictions of $\underline{H}_o^g$. The components of equations (1) – (3) are considered along the cylindrical coordinates (r, φ, z) with the z-axis is coinciding with the axis of the hollow jet. The model is acted by the inertia, pressure gradient, capillary and electromagnetic forces.

The hydromagnetic fundamental equations appropriate for studying the stability of the fluid model under consideration are the combination of the pure hydrodynamic equations and those of Maxwell concerning the electromagnetic theory. These equations may be given as follows.

In the gas cylinder

$$\nabla \Lambda \underline{H}^g = 0 \qquad \text{(There is no current)} \tag{4}$$

$$\nabla . \underline{H}^g = 0 \tag{5}$$

In the liquid region,

$$\rho\left(\frac{\partial}{\partial t} + (\underline{u}.\nabla)\right)\underline{u} = -\nabla P + \mu\,(\nabla \Lambda \underline{H})\Lambda \underline{H} \tag{6}$$

$$\nabla . \underline{u} = 0 \tag{7}$$

$$\nabla . \underline{H} = 0 \tag{8}$$

$$\frac{\partial \underline{H}}{\partial t} = \nabla \Lambda (\underline{u} \Lambda \underline{H}) - \nabla \Lambda (\eta \nabla \Lambda \underline{H}) \quad (9)$$

Along the gas – liquid interface,

$$P_s = -T (\nabla . \underline{N}) \quad (10)$$

With

$$(\nabla \cdot \underline{N}) = r_1^{-1} + r_2^{-1} \quad (11)$$

Here $\underline{H}$ and $\underline{H}^g$ are the magnetic field intensities in the gas and liquid regions, P_s the curvature pressure due to the capillary force, T the surface tension coefficient, $\underline{N}$ the outward unit vector normal to gas - liquid interface and indicates as r (the radial cylindrical coordinate) does, μ the magnetic permeability coefficient, while ρ, $\underline{u}$ and P are the liquid mass density, velocity vector and kinetic pressure.

For a small departure from the unperturbed state, based on the normal mode analysis technique, every variable quantity Q (r, 0, z, t) could be expanded as

$$Q(r, 0, z, t) = Q_o(r) + Q_1(r, 0, z, t) + \ldots\ldots\ldots \quad (12)$$

Here Q (r, 0, z, t) stands for $\underline{u}, P, \underline{H}, \underline{H}^g, \underline{N}$ and P_s with Q_o (r) is the value of Q (r, 0, z, t) in the unperturbed state, while Q_1(r, 0, z, t) is a small increment of Q (r, 0, z, t) due to perturbation. Based on the expansion (12), the perturbed radial distance of the gas cylinder may be expressed as

$$r = R_o + R_1 \quad (13)$$

With $R_1 = \varepsilon_0 \exp(ikz + \sigma t)$ (14)

is the elevation of the surface wave measured from the unperturbed level. Here k (real number) is the longitudinal wave number and σ is the growth rate.

Consequently, the linearized system of equations are solved and the required boundary conditions are applied, we finally obtained the dispersion relation

$$(\sigma + ikU)^2 \left[1 + \frac{\mu H_0^2}{\rho R_0^2}\left(\frac{xyK_0(y)}{GK_0(x)(\sigma + ikU)^2} - \frac{x\beta^2 K_1(x)}{K_0(x)(\sigma + ikU)^2}\right)\right]$$

$$= \frac{T}{\rho R_0^3}\left[1 + \frac{\mu H_0^2}{\rho R_0^2}\frac{x^2 K_1(y)}{GK_1(x)(\sigma + ikU)^2}\right]\frac{xK_1(x)}{K_0(x)}(1 - x^2)$$

(15)

where

$$x = kR_0, \qquad y^2 = x^2 + \frac{R_0^2}{\eta(\sigma+ikU)}\left[(\sigma+ikU)^2 + \frac{\mu H_0^2 x^2}{\rho R_0^2}\right] \tag{16}$$

$$G = -xI_0(x)K_0^{'}(y) + yK_0(x)I_0^{'}(y) \tag{17}$$

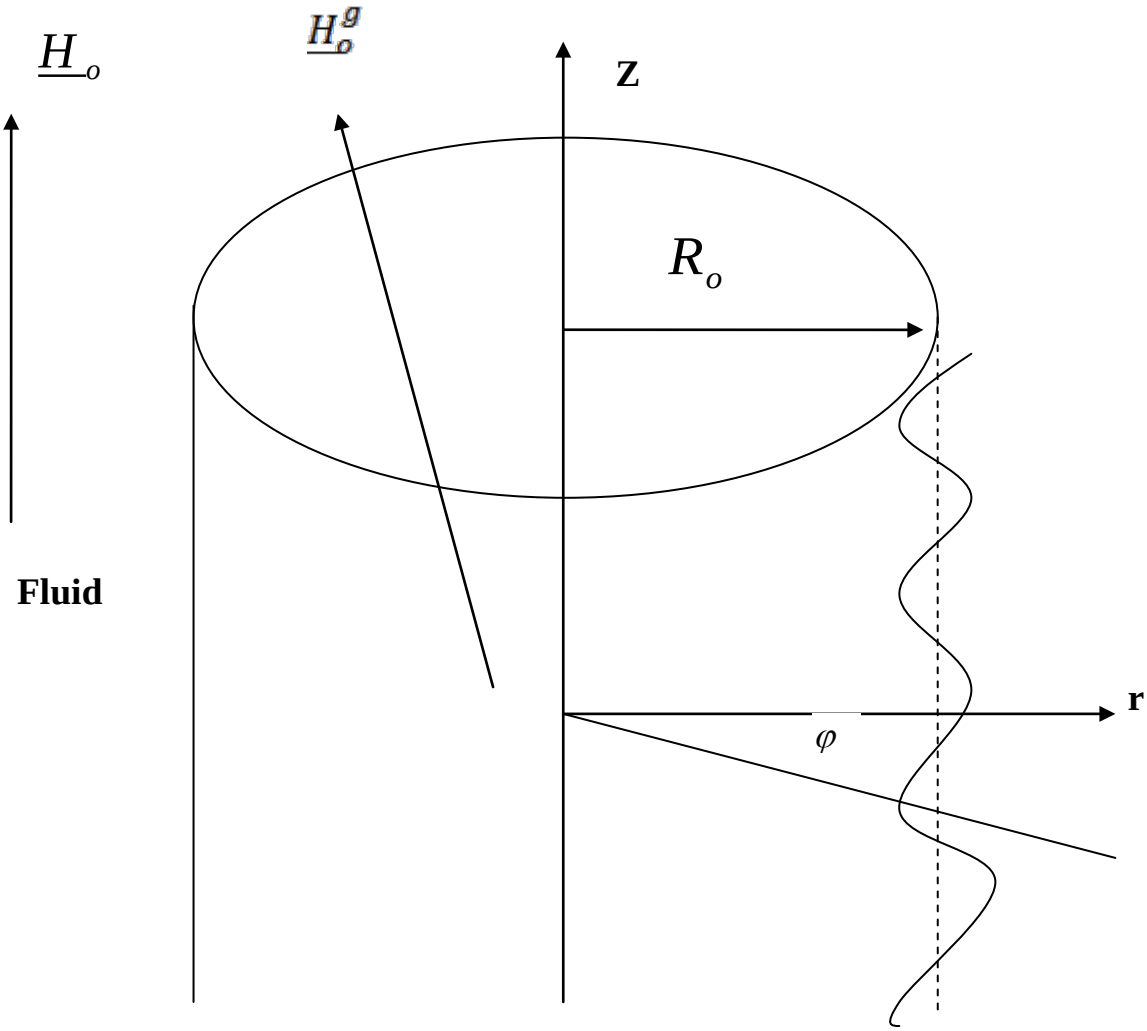

Figure 0: Sketch for MHD Hollow Jet

It is found more convenient to formulate the dispersion relation (15) in the dimensionless form

$$n^2\left[1 + \frac{\xi^2 xyK_0(y)}{n^2 GK_0(x)} - \frac{\xi^2 x\beta^2 K_1(x)}{n^2 K_0(x)}\right] = \left[1 + \frac{\xi^2 x^2 K_1(y)}{n^2 GK_1(x)}\right]\left[\frac{xK_1(x)(1-x^2)}{K_0(x)}\right]$$

(18)

with $$y^2 = x^2 + \frac{1}{n\zeta}(n^2 + x^2\xi^2) \quad (19)$$

where

$$n = (\sigma + ikU)\sqrt{\frac{\rho R_0^3}{T}}, \qquad \xi = \frac{H_0}{H_s} \quad (20)$$

$$H_s = \sqrt{\frac{T}{\mu R_0}}, \qquad \zeta = \eta\sqrt{\frac{\rho}{TR_0}} \quad (21)$$

3. Numerical Simulation Models using ANN

Artificial Neural Network (ANN) is a numerical model depends on a certain number of neurons in different layers. Every neuron acts very closely to the real neuron of the human brain. Each layer has a different function than the others. The input layer with its neurons gets the information from the external world (given data), while the hidden layers are working as detectors of these data. The output layer is the final layer of the network and it produces the required results. Neuralyst software, Shin [21] is used to design the ANN models in the present work.

3.1 Simulation Cases

To fully investigate the effect of ζ = 0.5, 1.0, 1.5, 2.0, 2.5, and 3.0 on σ^* for different values of position X and certain values of β, U^* and ξ eight numerical models, using ANN, are designed in this study. The developed simulation models used some solution outputs obtained from the analytic solution to design the ANN models.

3.2 Numerical Models Design

To design ANN models to simulate and predict σ^*, the input and output variables have to be determined. Table 1 shows the eight neural network models. Table 1 shows the eight neural network models with its associate input and output variables.

Several ANN models are tested for all numerical models to finally choose the best networks design to simulate, very accurately, the effect of ζ and position X on σ^* based on minimizing the Root Mean Square Error (RMS-Error). The training procedure for the developed ANN models, in the current study, uses some rows of the data from the analytic results to let the ANN understands the behavior. After sitting finally the NN models, these models are used to predict σ^* for different values of ζ at any X. Table 2 presents the final design of the developed ANN models for the eight models. The structure of the eight models is chosed to

minimize the RMS-Error to achieve accepted accuracy represented by maximum percentage relative error (Max PRE %).

Table 1: Key Input and Output Variables for Neural Network Models.

ANN Models	Input Variables		Output
ANN 1 (β = 0.5, $U^* = 0$ and ξ = 0.5)	ζ	X	σ^*
ANN 2 (β = 1.5, $U^* = 0$ and ξ = 0.5)			
ANN 3 (β = 3.0, $U^* = 0$ and ξ = 0.5)			
ANN 4 (β = 5.0, $U^* = 0$ and ξ = 0.5)			
ANN 5 (β = 0.5, $U^* = 0$ and ξ = 1.5)			
ANN 6 (β = 1.5, $U^* = 0$ and ξ = 1.5)			
ANN 7 (β = 0.5, $U^* = 0.5$ and ξ = 0.5)			
ANN 8 (β = 1.5, $U^* = 0.5$ and ξ = 0.5)			

Table 2: The Designed ANN Models.

ANN Models	No. of layers	No. of Neurons in each layer					
		Input Layer	First Hidden	Second Hidden	Third Hidden	Fourth Hidden	Output Layer
ANN 1	6	2	4	4	4	4	1
ANN 2	6	2	4	4	4	4	1
ANN 3	6	2	4	4	4	4	1
ANN 4	6	2	4	4	4	4	1
ANN 5	6	2	4	4	4	4	1
ANN 6	5	2	4	4	4	-	1
ANN 7	5	2	4	4	4	-	1
ANN 8	4	2	4	4	-	-	1

The parameters of the various network models developed in the current study for the different simulation models can be described with their tasks as follows:

Learning Rate (LR): determines the magnitude of the correction term applied to adjust each neuron's

weights during training process = 1 in the current study.

Momentum (M): determines the "life time" of a correction term as the training process takes place = 0.9 in the current study.

Training Tolerance (TRT): defines the percentage error allowed in comparing the neural network output to the target value to be scored as "Right" during the training process (for all models TRT=0.001).

Testing Tolerance (TST): it is similar to Training Tolerance, but it is applied to the neural network outputs and the target values only for the test data (for all models TST=0.003)

Input Noise (IN): provides a slight random variation to each input value for every training epoch = 0 in the current study.

Function Gain (FG): allows a change in the scaling or width of the selected function = 1 in the current study.

Scaling Margin (SM): adds additional headroom, as a percentage of range, to the rescaling computations used by Neuralyst Software, Shin [21], in preparing data for the neural network or interpreting data from the neural network = 0.1 in the current study.

Table 3 presents the accuracy achieved for the eight models in the current study presented by RMS-Error and Max PRE %. The term PRE showed in the table referred to percentage relative error and is computed based on equation 41 as follows:

$$PRE = (\text{Absolute Value } (ANN\_PR - AMV)/AMV)*100 \quad (41)$$

Where :

ANN_PR : Predicted results using the developed ANN model

AMV : Actual Measured Value

Table 3: The RMS-Error and Max PRE % for the Developed Models

ANN Models	ANN 1	ANN 2	ANN 3	ANN 4	ANN 5	ANN 6	ANN 7	ANN 8
RMS-Error	0.0006	0.0007	0.0035	0.0011	0.0012	.0076	0.0006	0.002
Max PRE %	1.366	1.2049	0.5277	0.1559	0.2163	1.2819	1.3614	1.2635

3.3 Numerical Simulation Results and Discussions

Numerical results using ANN technique are presented in Figures 1-8 for the eight ANN models to simulate and predict the effect of ζ = 0.5, 1.0, 1.5, 2.0, 2.5, and 3.0 on σ^* for different values of position X. Figures 1a-8a show the training and verification for the eight developed models. It is clear from these figures that the designed models understand the behavior very well and the verification curves in these figures with RMS-Error and Max PRE prove that. The designed models are used to predict the effect of ζ on σ^* without the need to go through the analytic solution as shown in Figures 1b-8b.

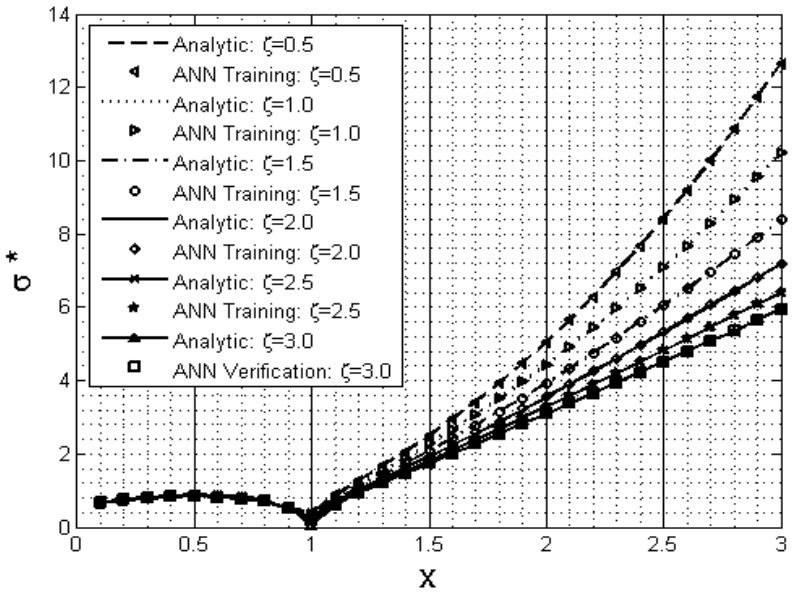

(a)

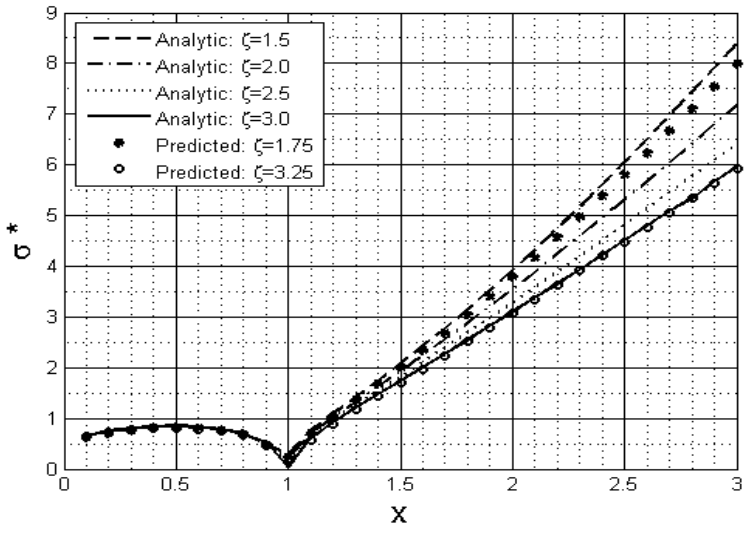

(b)

Figure 1: Stable and unstable domains for β = 0.5, $U^* = 0$ and ξ = 0.5

(a) Analytic, Training ANN and Verification ANN (b) Analytic and Prediction ANN

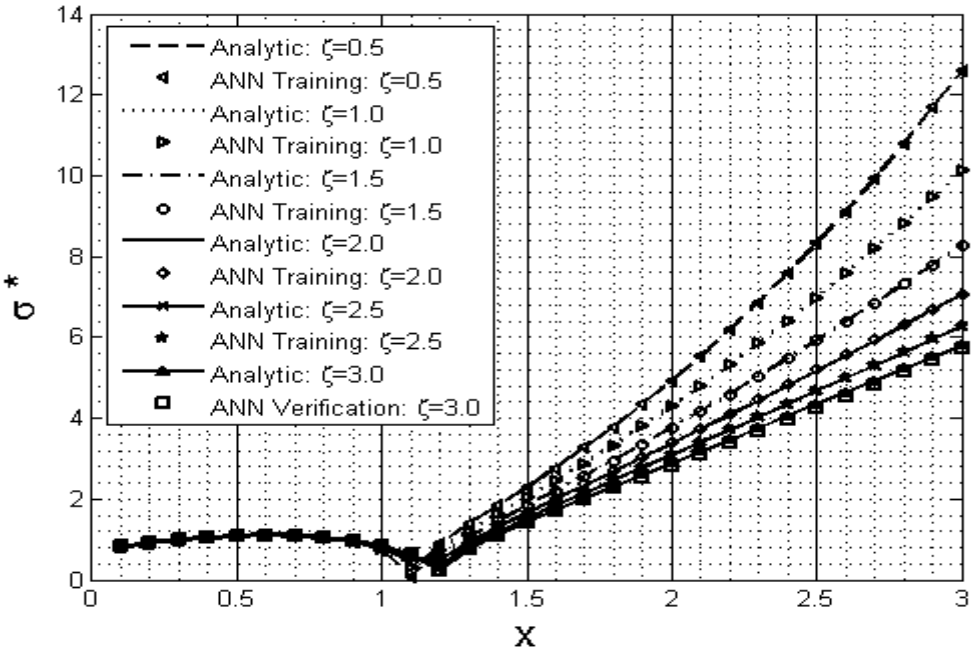

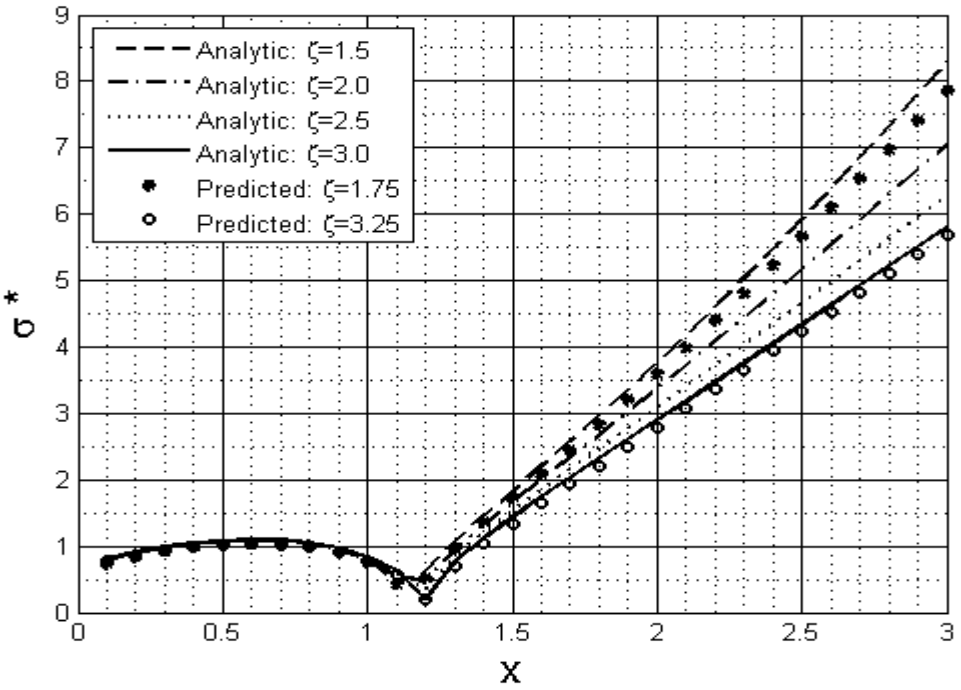

(a)

(b)

Figure 2: Stable and unstable domains for β = 1.5, $U^* = 0$ and ξ = 0.5

(a) Analytic, Training ANN and Verification ANN (b) Analytic and Prediction ANN

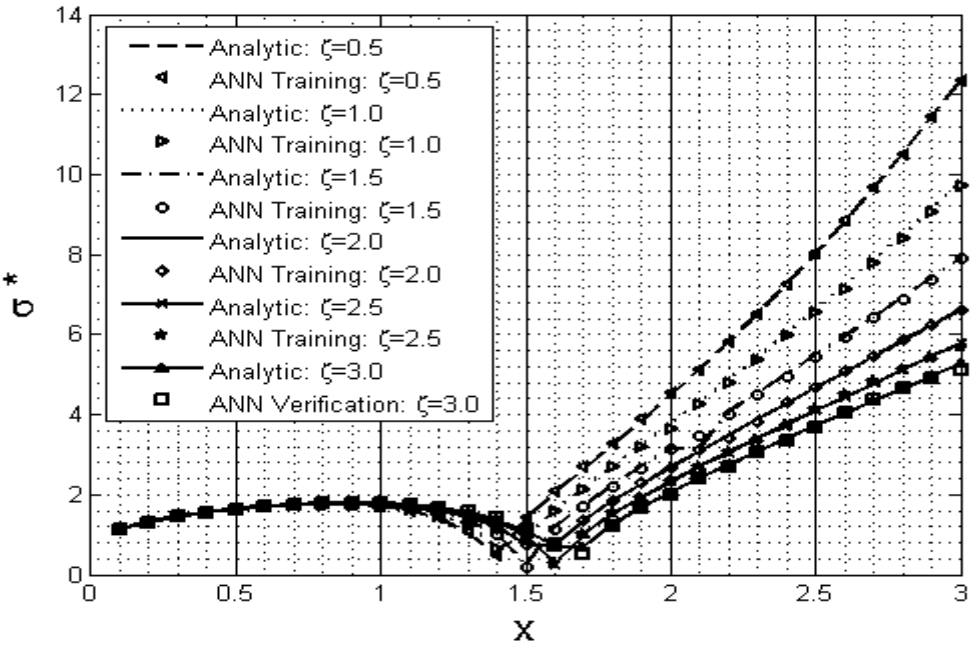

(a)

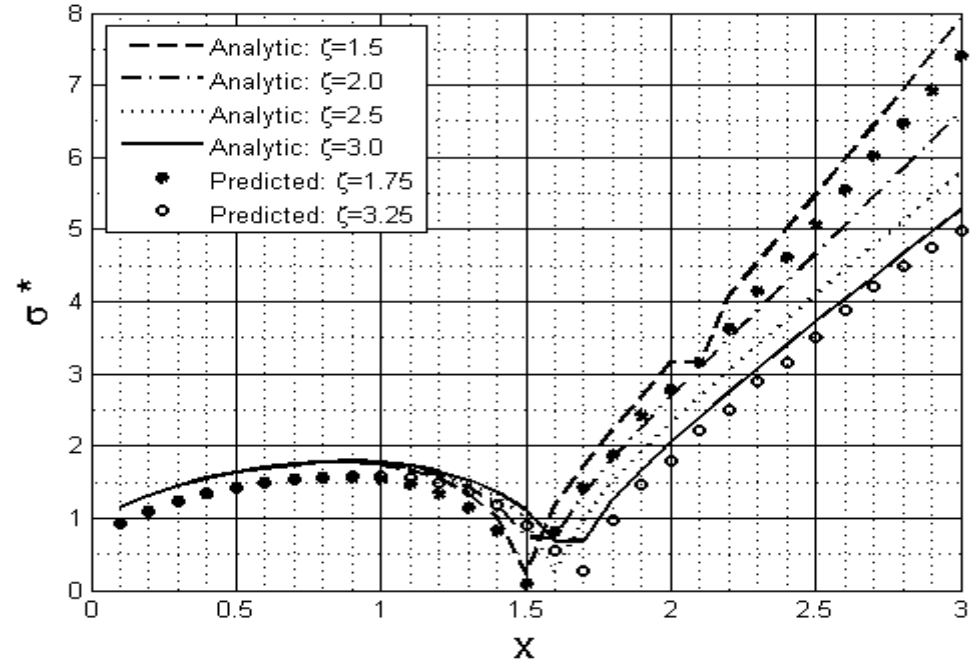

(b)

Figure 3: Stable and unstable domains for β = 3, $U^* = 0$ and ξ = 0.5

(a) Analytic, Training ANN and Verification ANN (b) Analytic and Prediction ANN

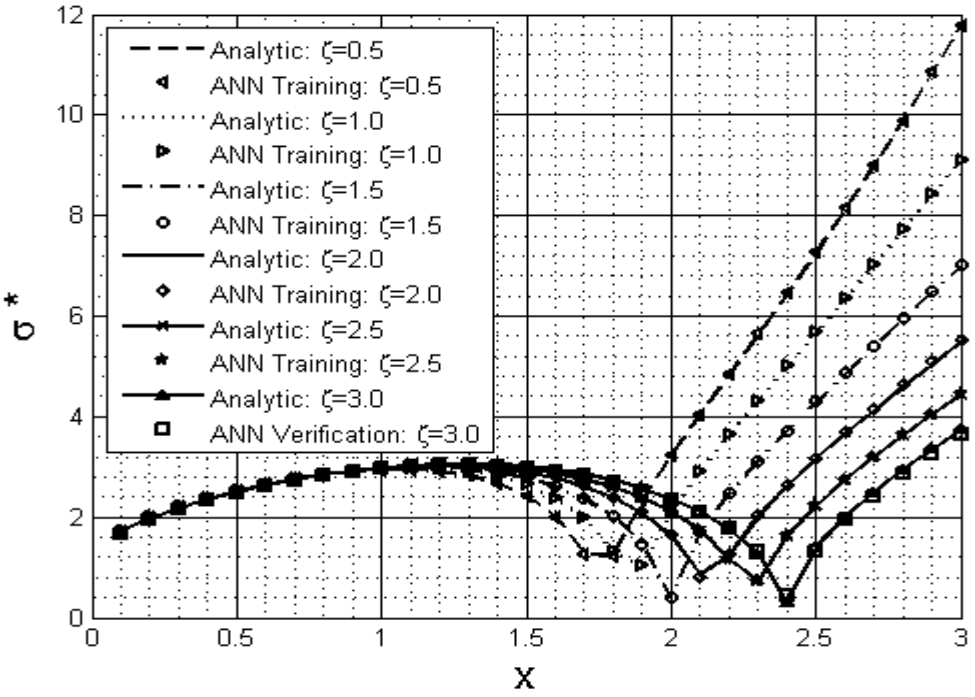

(a)

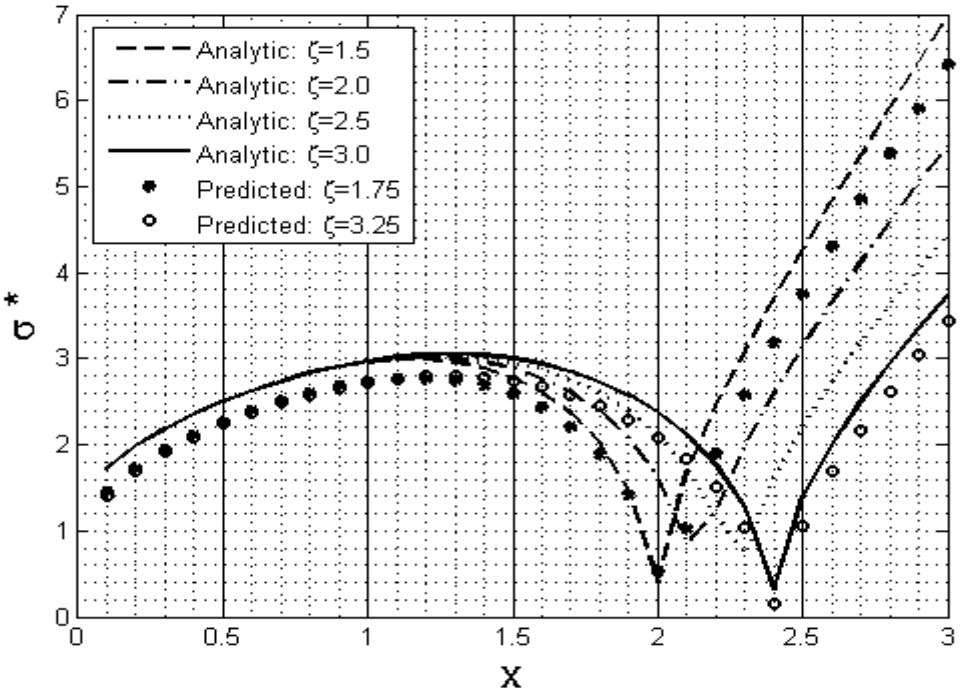

(b)

Figure 4: Stable and unstable domains for β = 5, $U^* = 0$ and ξ = 0.5

(a) Analytic, Training ANN and Verification ANN (b) Analytic and Prediction ANN

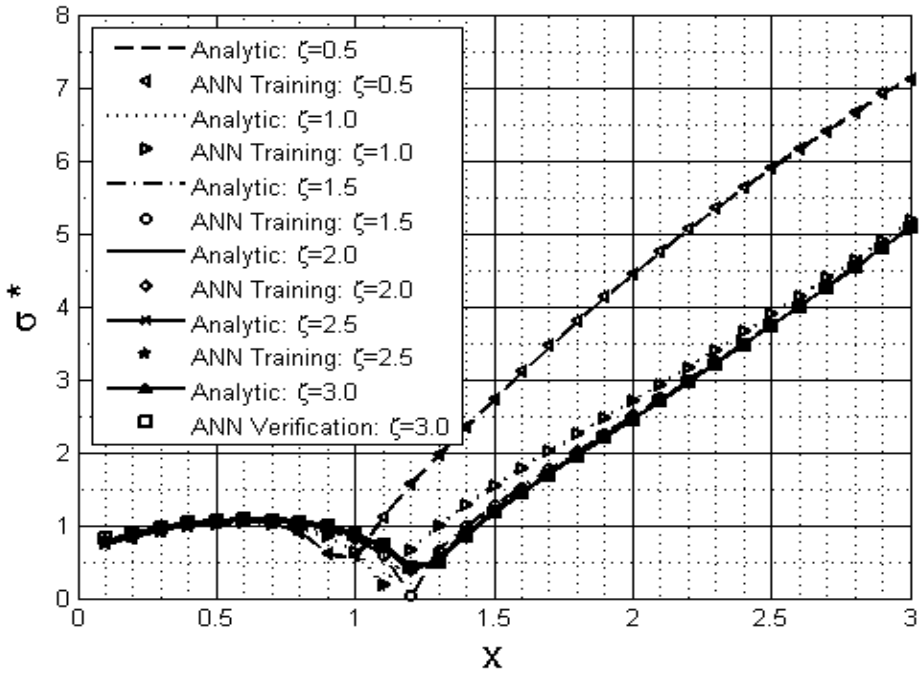

(a)

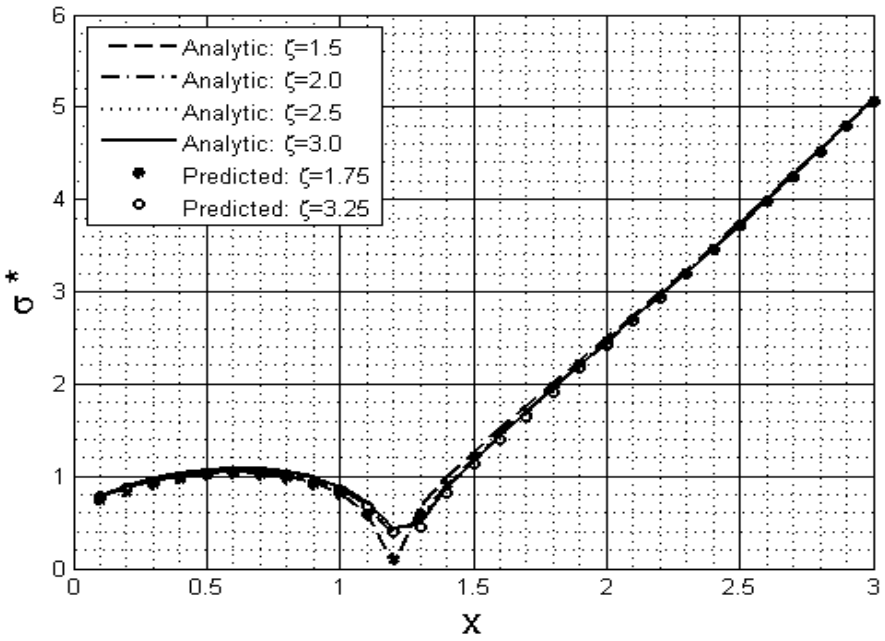

(b)

Figure 5: Stable and unstable domains for β = 0.5, $U^* = 0$ and ξ = 1.5

(a) Analytic, Training ANN and Verification ANN (b) Analytic and Prediction ANN

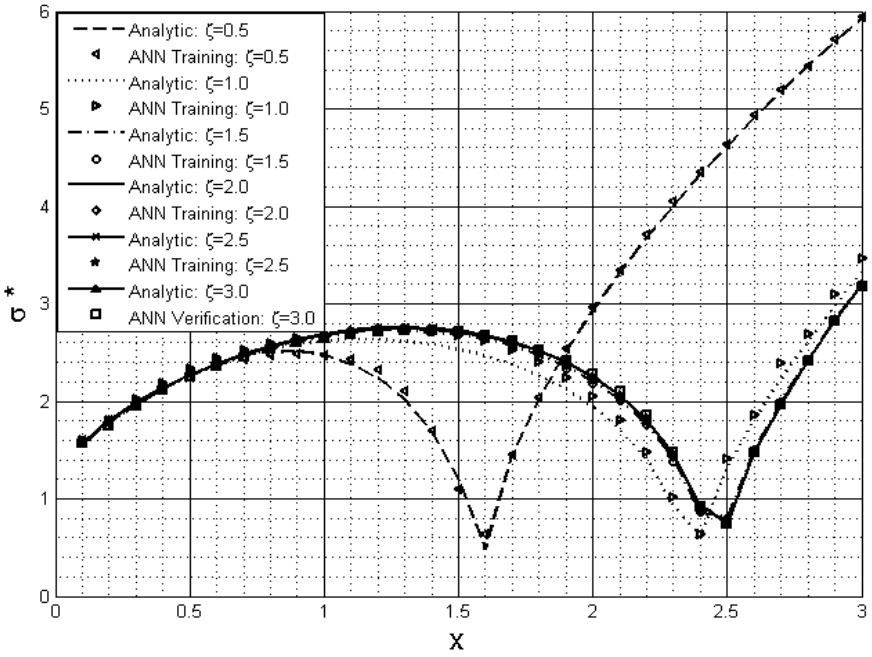

(a)

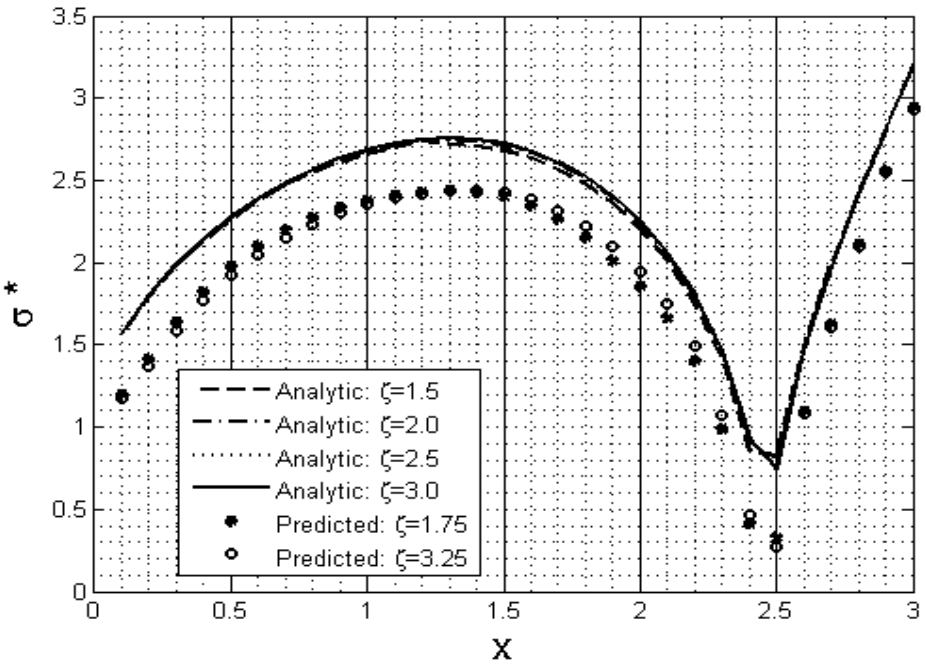

(b)

Figure 6: Stable and unstable domains for β = 1.5, $U^* = 0$ and ξ = 1.5

(a) Analytic, Training ANN and Verification ANN (b) Analytic and Prediction ANN

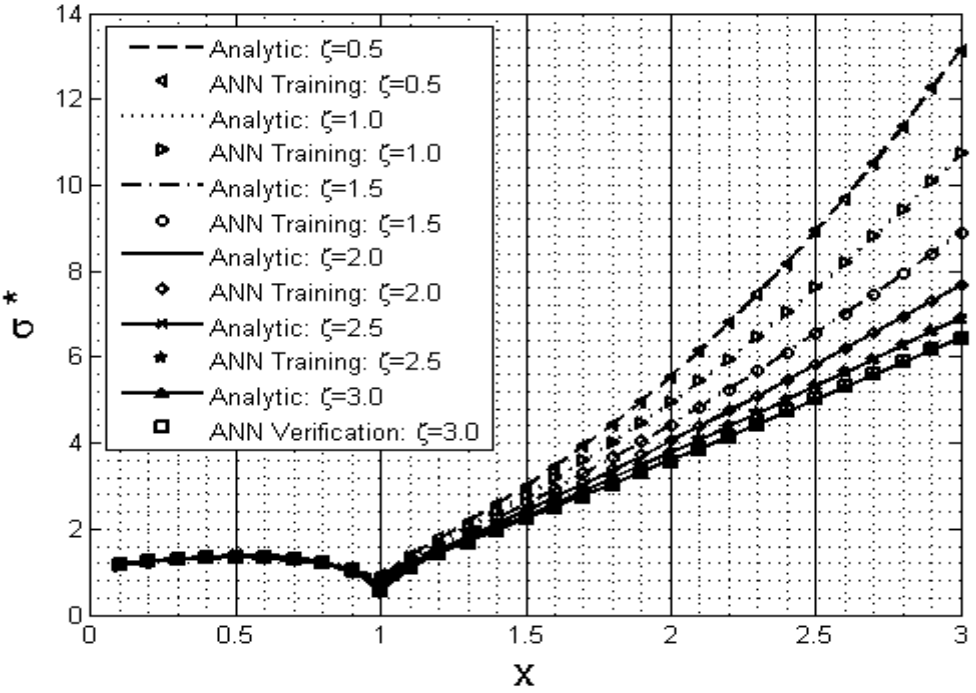

(a)

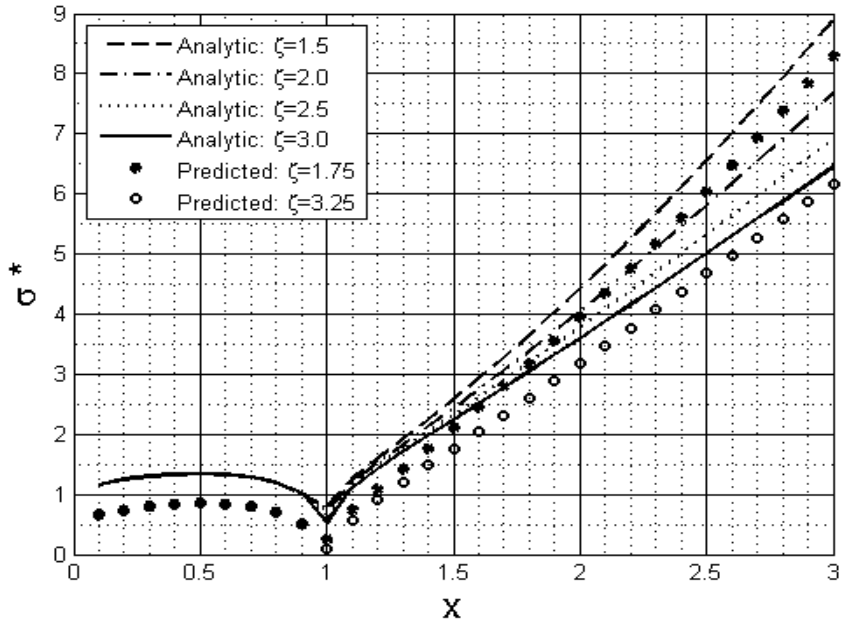

(b)

Figure 7: Stable and unstable domains for β = 0.5, $U^* = 0.5$ and ξ = 0.5

(a) Analytic, Training ANN and Verification ANN (b) Analytic and Prediction ANN

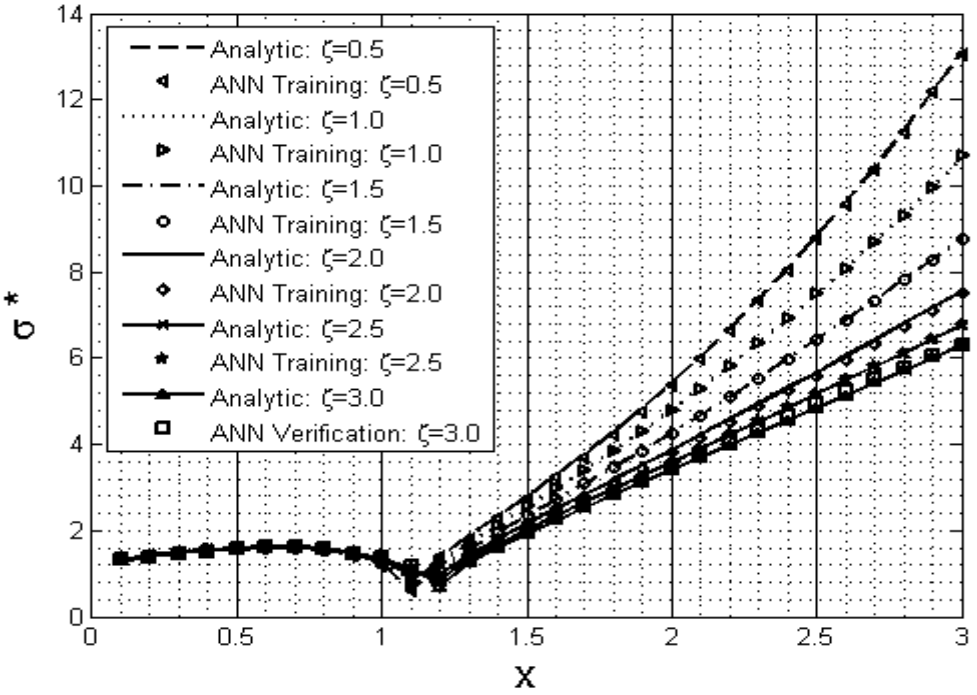

(a)

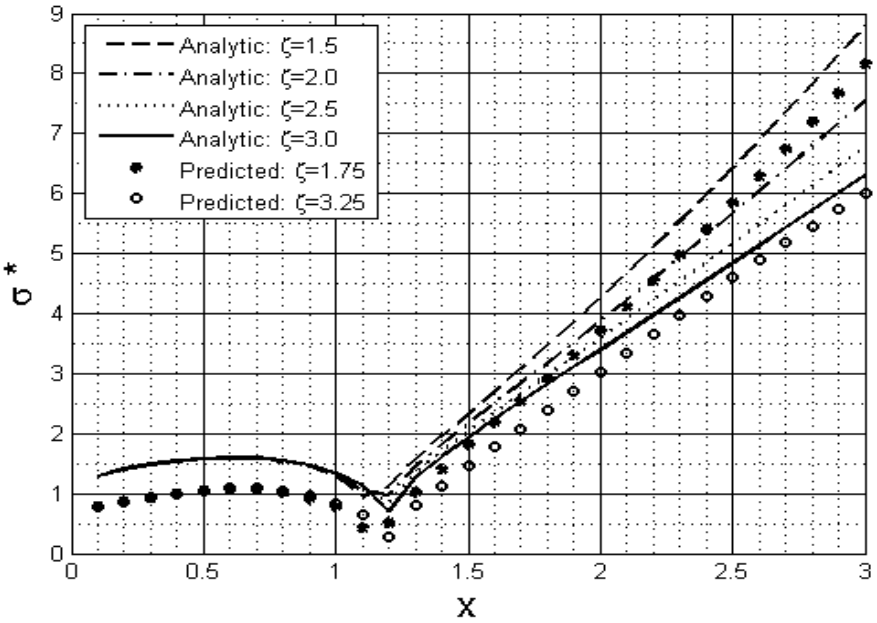

(b)

Figure 8: Stable and unstable domains for β = 1.5, $U^* = 0.5$ and ξ = 0.5

(a) Analytic, Training ANN and Verification ANN (b) Analytic and Prediction ANN

4. Conclusion

From the foregoing discussions of MHD stability a resistive hollow jet endowed with surface tension we may formulate the following conclusions.

1. The hollow jet is capillary unstable only in the axisymmetric mode while it is stable in the rest, due to the fact that the gradient pressure force is predominant over that of the curvature pressure.

2. If the fluid is with infinite resistivity ($\eta \to \infty$), the electromagnetic force is stabilizing influence on the capillary instability of the cylindrical resistive hollow jet.

3. If the fluid is with finite resistivity, the electromagnetic force is stabilizing or destabilizing according to the restrictions. In fact, as we see from the figures, it is found that the resistivity factor has a stabilizing tendency, so it decreases the MHD unstable domains and simultaneously it increase those of stability.

4. If the fluid is perfectly conducting ($\eta \to 0$), the magnetic field exerts an influence that endows the fluid a sort of rigidity. The magnetic field has a strong stabilizing influence, which may cause shrinking the capillary destabilizing effect. Moreover, above a certain high value of the acting basic magnetic field the capillary instability is completely suppressed and stability arises.

Based on the output results of the developed ANN models in this study, the following can be concluded:

1. The developed ANN models are very smarting in understanding the effect of ζ on σ^* for different values of position X.

2. The designed ANN models can successfully capable of direct predicting the response behavior of σ^* for different values of ζ at any position X without the need to go through the analytic solution.

References

[1]. Abramowitz M and Stegun I (1970).Handbook of Mathematical Functions. Dover Publ., N.Y.

[2]. Abdeen, M A, Neural Network Model for predicting Flow Characteristics in Irregular Open Channel, Scientific Journal, Faculty of Engineering-Alexandria University, 40(4), (2001) 539.

[3]. Abdeen, M A, Development of Artificial Neural Network Model for Simulating the Flow Behavior in Open Channel Infested by Submerged Aquatic Weeds, Journal of Mechanical Science and technology, KSME Int. J., 20(10) (2006)1.

[4]. Abdeen, MA, Predicting the Impact of Vegetations in Open Channels with Different Distributeries Operations on Water Surface Profile Using Artificial Neural Networks, Journal of Mechanical Science and Technology (KSME Int. J.) 22, (2008)1830.

[5]. Abdeen MA, Hasan AA, MHD Stability of Streaming Jet using Artificial Intelligence Technique", Journal of Mechanics, 2012, 28(3), 391.

[6]. Abdeen MA and Bichir SM, Analysis of Simply Supported thin FGM Rectangular Plate Resting on Fluid Layer", Arabian Journal Of Science and Engineering (AJSE), 38, (2013)3267.

[7]. Chandrasekhar, S: Hydrodynamic and Hydromagnetic Stability. Dover, New York (1981)

[8]. Chandrasekhar, S, Fermi, E: Problems of gravitational stability in the presence of a magnetic field. Astrophys J. 118, (1953)116.

[9]. Gaafar MS, Abdeen MA, Marzouk SY, Structural Investigation and Simulation of Acoustic Properties of Some Tellurite Glasses Using Artificial Intelligence Technique, Journal of Alloys and Combounds, 509 (2011), 3566.

[10]. Hasan, AA, Electrogravitational stability of oscillating streaming fluid cylinder, Physica B. 406(2), (2011) 234.

[11]. Hasan, AA, Electrogravitational stability of oscillating streaming dielectric compound jets ambient with a transverse varying electric field, Boundary Value Problems,2011(31),(2011)1.

[12]. Hasan, AA, Electrogravitational stability of oscillating streaming fluid cylinder. J Appl Mech ASME. 79(2),(2012)1.

[13]. Hasan, AA, Hydromagnetic instability of streaming jet pervaded internally by varying transverse magnetic field. Mathematical Problems in Engineering, (2012)1.

[14]. Hasan, AA, Abdelkhalek, RA, Magnetogravitodynamic Stability of Streaming Fluid Cylinder Under The Effect of Capillary Force, Boundary Value Problems, 2013(48)1.

[15]. Hasan, AA, , Electrogravitational stability of streaming compound jets, International Journal of Biomathematics, 2015, Accepted.

[16]. Hodhod H and Abdeen MA, Simulation and Prediction for the Effect of Natural and Steel Fibers on the Performance of Concrete using Experimental Analyses and Artificial Neural networks Numerical Modeling, KSCE, Journal of Civil Engineering, 15(8), (2011)1373.

[17]. El-Mallawany M, Gaafarb MS, Abdeen MA, Marzouk SY, Simulation of acoustic properties of some tellurite glasses**,** Ceramics International, 40(2014)7389.

[18]. Radwan, AE, Hasan, AA, Axisymmetric electrogravitational stability of fluid cylinder ambient with transverse varying oscillating field, (IAENG). Int J Appl Math.38(3), (2008)113.

[19]. Radwan, AE, Hasan, AA, Magnetohydrodynamic stability of selfgravitationalfluid cylinder. Appl Math Model.33(4), (2009) 2121.

[20]. Rayleigh J, "The Theory of Sound" Vols I&II, Dover Publ., N.Y. (1945).

[21]. Shin, Y. Neuralyst^{TM} User's Guide. Neural Network Technology for Microsoft Excel. Cheshire Engineering Corporation Publisher (1994).